Acta Mechanica 156, 145–161 (2002)

ACTA MECHANICA

Green's function approach to unsteady thermal stresses in an infinite hollow cylinder of functionally graded material

K.-S. Kim, Incheon, Korea, and **N. Noda,** Hamamatsu, Japan

(Received July 30, 2001; revised September 5, 2001)

Summary. A Green's function approach based on the laminate theory is adopted for solving the two-dimensional unsteady temperature field (r, z) and the associated thermal stresses in an infinite hollow circular cylinder made of a functionally graded material (FGM) with radial-directionally dependent properties. The unsteady heat conduction equation is formulated as an eigenvalue problem by making use of the eigenfunction expansion theory and the laminate theory. The eigenvalues and the corresponding eigenfunctions obtained by solving an eigenvalue problem for each layer constitute the Green's function solution for analyzing the unsteady temperature. The associated thermoelastic field is analyzed by making use of the thermoelastic displacement potential function and Michell's function. Numerical results are carried out and shown in figures.

1 Introduction

A functionally graded material (FGM) is characterized by continuously changing material properties due to a graded composition from one surface to the other surface. For non-homogeneous materials such as FGMs, the governing equations of the unsteady temperature field and the associated thermoelastic field in an infinite hollow circular cylinder are presented in complex forms according to position dependent material properties. Therefore, the theoretical treatment for these equations is difficult, and an exact solution is almost impossible to obtain.

Tanigawa [1] reviewed some basic problems for nonhomogeneous structural materials. Obata and Noda [2] discussed unsteady thermal stresses in a functionally gradient material (FGM) plate, and Obata et al. [3] analyzed the two-dimensional unsteady thermal stress in a FGM hollow circular cylinder by using the Laplace transformation and the perturbation method. Ootao and Tanigawa [4] treated three-dimensional transient thermal stress analysis in a nonhomogeneous hollow sphere, and Tanigawa et al. [5] studied transient heat conduction and thermal stress problems of a nonhomogeneous plate by use of the Laplace transformation and multi-layers approximation approach.

On the other hand, the Green's function approach for homogeneous materials has been well known. Carslaw and Jaeger [6] explained the use of Green's functions in the solution of the equation of conduction in their book, Parkus [7] described the Green's function for temperature, and Boley and Weiner [8] discussed the Green's function technique in their book. However, there is little work about Green's function for nonhomogeneous materials such as FGMs. Diaz and Nomura [9] used a Green's function approach for two-dimensional elastic problems. Nomura and Sheahen [10] used a Green's function based on the Galerkin method to analyze steady thermal stresses in a two-dimensional FGM plate. Kim and Noda [11] used a Green's function based on the Galerkin method to analyze the three-dimensional transient temperature for thermal stresses of a functionally graded material. Kim and Noda [12] used a Green's function based on the laminate theory to analyze the three-dimensional heat conduction equation of functionally graded materials.

Many workers have studied the thermal stress problems in homogeneous cylinders subjected to nonstationary heating, because there are many practical applications in modern engineering. Many kinds of transient thermal stress problems in homogeneous cylinders are treated in several books, e.g., by Parkus [7], Boley and Weiner [8], and Nowacki [13]. But there is little work done to determine the thermal stresses in nonhomogeneous cylinders such as FGM cylinders. Obata and Noda [14] discussed steady thermal stresses in a hollow circular cylinder and a hollow sphere of FGM. Ootao, Akai, and Tanigawa [15] studied three-dimensional transient thermal stresses in a nonhomogeneous hollow circular cylinder due to a moving heat source. Tanigawa et al. [16] treated the one-dimensional transient thermal stress problem for nonhomogeneous hollow circular cylinders.

In this paper, we discuss the Green's function technique based on the laminate theory for an infinite hollow FGM cylinder subjected to temperature variations along both r- and z-axis. Since almost all FGMs are materials whose compositions are dependent on a function of one-directional position from a metal surface to a ceramic surface, it is assumed that the thermal properties of FGMs are dependent on the one-directional position. As for the analytical treatment, introducing the analytical technique for the laminate theory and taking into account the bounds that the number of laminae becomes sufficiently large, the unsteady temperature solution for a two-dimensional FGM hollow circular cylinder with an infinite length is formulated by the Green's function approach based on the laminate theory. An approximate solution of the eigenfunction expansion method for each layer is substituted into the governing equation to yield an eigenvalue problem. The eigenvalues and the corresponding eigenfunctions resulting by solving an eigenvalue problem for each layer constitute the Green's function solution for obtaining the two-dimensional unsteady temperature distribution. The associated thermoelastic field is analyzed by making use of the thermoelastic displacement potential function [17] and Michell's function [18].

As an example, a FGM hollow circular cylinder with an infinite length, which is made of zirconium oxide and titanium alloy, is selected. Numerical results, such as the temperature distribution and the thermal stress distribution, are shown in the figures.

2 Analysis

We consider the two-dimensional unsteady temperature field and the associated thermoelastic field in an infinite hollow circular cylinder (r, z) made of a functionally graded material whose thermal properties vary with the radial coordinate r. The inside and outside radii of the hollow circular cylinder are r_a and r_b, respectively, and it has an infinite length in z-direction. We assume the thermal condition that the inside and outside surface are heated to $T_0 + T_a(z)$ and $T_0 + T_b(z)$, where $T_0, T_a(z)$ and $T_b(z)$ are the initial temperature, and an arbitrary even function at $r = r_a$ and $r = r_b$, respectively. Assuming that the number of laminae becomes sufficiently large and the thermal properties of each layer are constants, we consider a laminated medium consisting of L layers in the temperature field and the associated thermoelastic field.

2.1 Two-dimensional steady temperature

Assuming that the thermal properties are dependent on the r-directional position and that the temperature is independent of the hoop direction position, the solution of the steady-state heat conduction equation for the i-th layer is assumed to be [19]:

$$T_i^s(r,z) = \int_0^\infty \{I_0(\beta r)\,A_i + K_0(\beta r)\,B_i\}\,\cos(\beta z)\,d\beta\,, \tag{1}$$

where $T_i^s\big(=T_i'(r,z,t)-T_0\big)$ and β are the temperature difference from the initial state and a parameter, respectively.

Thus, we can obtain the steady state solution $T_i^s(r,z)$ by using the continuous conditions of temperature and heat flux at the interfaces, and the nonhomogeneous boundary conditions at the inside and outside surface as:

$$T_1^s = T_a(z) \quad \text{at} \quad r = r_a\,, \tag{2.1}$$

$$T_i^s = T_{i+1}^s \quad \text{at} \quad r = r_i\,, \qquad i = 1,2,\ldots\,(L-1)\,, \tag{2.2}$$

$$k_i\,\frac{\partial T_i^s}{\partial r} = k_{i+1}\,\frac{\partial T_{i+1}^s}{\partial r} \quad \text{at} \quad r = r_i\,, \qquad i = 1,2,\ldots,(L-1)\,, \tag{2.3}$$

$$T_L^s = T_b(z) \quad \text{at} \quad r = r_b\,, \tag{2.4}$$

where k_i is the thermal conductivity of the i-th layer.

2.2 Two-dimensional unsteady temperature

The governing equations of the unsteady-state problem in the absence of a heat source and the initial conditions for each layer are given as

$$\nabla^2\theta_i = \frac{1}{\lambda_i}\,\frac{\partial\theta_i}{\partial t} \quad \text{at} \quad r_{i-1} \le r \le r_i\,, \qquad i = 1,2,\ldots,L \tag{3}$$

$$\theta_i(r,z,0) = F_i(r,z) = -T_i^s(r,z) \quad \text{at} \quad r_{i-1} \le r \le r_i\,, \qquad i = 1,2,\ldots,L \tag{4}$$

where

$$\nabla^2 = \frac{\partial^2}{\partial r^2} + \frac{\partial}{r\partial r} + \frac{\partial^2}{\partial z^2}\,,$$

and θ_i and λ_i are the temperature change and the thermal diffusivity of i-th layer, respectively. Using the eigenfunction expansion theory and the separation of variables, we can obtain the solution of Eq. (3) as [19]

$$\theta_i(r,z,t) = \sum_{m=1}^{\infty}\int_0^\infty c_m(\beta)\,\varphi_{im}(\alpha_m,r)\,\cos(\beta z)\,e^{-(\alpha_m^2+\lambda_i\beta^2)\,t}\,d\beta\,, \quad \text{at} \quad r_{i-1} \le r \le r_i\,, \qquad i = 1,2,\ldots,L\,, \tag{5}$$

where $c_m(\beta)$ are constants to be evaluated. Substituting Eq. (5) into Eq. (3) yields an eigenvalue problem,

$$\frac{\partial}{r\partial r}\left\{r\,\frac{\partial\varphi_{im}}{\partial r}\right\} + \frac{\alpha_m^2}{\lambda_i}\,\varphi_{im} = 0 \quad \text{at} \quad r_{i-1} \le r \le r_i\,, \qquad i = 1,2,\ldots,L\,, \tag{6}$$

where α_m and φ_{im} are eigenvalues and eigenfunctions to be evaluated, respectively. Applying the initial conditions of Eq. (4) to Eq. (5), the coefficients $c_m(\beta)$ are obtained as

$$c_m(\beta) = \frac{2}{\pi}\frac{1}{N_m}\sum_{j=1}^{L}\frac{k_j}{\lambda_j}\int_0^{\infty}\int_{r=r_{j-1}}^{r_j} r' F_j(r',z')\,\varphi_{jm}(r')\,\cos(\beta z')\,dr'\,dz'\,, \tag{7}$$

where the norm N_m is defined as

$$N_m = \sum_{j=1}^{L}\frac{k_j}{\lambda_j}\int_{r=r_{j-1}}^{r_j} r'\varphi_{jm}^2(r')\,dr'\,. \tag{8}$$

Substituting Eq. (7) into Eq. (5) and introducing Green's function, the solution of Eq. (3) yields

$$\theta_i(r,z,t) = \sum_{j=1}^{L}\int_0^{\infty}\int_{r=r_{j-1}}^{r_j} r' G_{ij}(r,z,t\,|\,r',z',t')|_{t'=0}\,F_j(r',z')\,dr'\,dz'\,, \tag{9}$$

where $G_{ij}(r,z,t\,|\,r',z',t')|_{t'=0}$ is defined as

$$G_{ij}(r,z,t\,|\,r',z',t')|_{t'=0} = \frac{2}{\pi}\sum_{m=1}^{\infty}\frac{1}{N_m}\frac{k_j}{\lambda_j}\,\varphi_{im}(r)\,\varphi_{jm}(r')\int_0^{\infty}\cos(\beta z)\,\cos(\beta z')\,e^{-(\alpha_m^2+\lambda_i\beta^2)t}\,d\beta\,. \tag{10}$$

2.3 *Determination of eigenfunctions and eigenvalues*

The general solution φ_{im} of Eq. (6) can be written as [19]:

$$\varphi_{im}(r) = C_{im}J_0\left(\frac{\alpha_m}{\sqrt{\lambda_i}}\,r\right) + D_{im}Y_0\left(\frac{\alpha_m}{\sqrt{\lambda_i}}\,r\right) \quad \text{at} \quad r_{i-1}\le r\le r_i\,, \qquad i=1,2,\ldots,L\,, \tag{11}$$

where J_0 and Y_0 denote the Bessel function of the first and second kind of order zero, respectively, and C_{im} and D_{im} are coefficients to be evaluated.

Applying the continuity conditions of temperature and heat flux at the interfaces to Eq. (11), the simultaneous equations for C_{im} and D_{im} are written in matrix form as

$$\begin{pmatrix} C_{im} \\ D_{im} \end{pmatrix} = \begin{bmatrix} P_{11} & P_{12} \\ P_{21} & P_{22} \end{bmatrix}\begin{pmatrix} C_{i+1,m} \\ D_{i+1,m} \end{pmatrix} \quad \text{at} \quad r=r_i\,, \qquad i=1,2,\ldots,L\,, \tag{12}$$

where

$$P_{11} = \frac{1}{DET}\left\{Y_1\left(\frac{\alpha_m}{\sqrt{\lambda_i}}\,r_i\right)J_0\left(\frac{\alpha_m}{\sqrt{\lambda_{i+1}}}\,r_{i+1}\right) - \frac{k_{i+1}}{k_i}\sqrt{\frac{\lambda_i}{\lambda_{i+1}}}\,Y_0\left(\frac{\alpha_m}{\sqrt{\lambda_i}}\,r_i\right)J_1\left(\frac{\alpha_m}{\sqrt{\lambda_{i+1}}}\,r_{i+1}\right)\right\},$$

$$P_{12} = \frac{1}{DET}\left\{Y_1\left(\frac{\alpha_m}{\sqrt{\lambda_i}}\,r_i\right)Y_0\left(\frac{\alpha_m}{\sqrt{\lambda_{i+1}}}\,r_{i+1}\right) - \frac{k_{i+1}}{k_i}\sqrt{\frac{\lambda_i}{\lambda_{i+1}}}\,Y_0\left(\frac{\alpha_m}{\sqrt{\lambda_i}}\,r_i\right)Y_1\left(\frac{\alpha_m}{\sqrt{\lambda_{i+1}}}\,r_{i+1}\right)\right\},$$

$$P_{21} = \frac{1}{DET}\left\{\frac{k_{i+1}}{k_i}\sqrt{\frac{\lambda_i}{\lambda_{i+1}}}\,J_0\left(\frac{\alpha_m}{\sqrt{\lambda_i}}\,r_i\right)J_1\left(\frac{\alpha_m}{\sqrt{\lambda_{i+1}}}\,r_{i+1}\right) - J_1\left(\frac{\alpha_m}{\sqrt{\lambda_i}}\,r_i\right)J_0\left(\frac{\alpha_m}{\sqrt{\lambda_{i+1}}}\,r_{i+1}\right)\right\},$$

$$P_{22} = \frac{1}{DET}\left\{\frac{k_{i+1}}{k_i}\sqrt{\frac{\lambda_i}{\lambda_{i+1}}}\, J_0\!\left(\frac{\alpha_m}{\sqrt{\lambda_i}}\, r_i\right) Y_1\!\left(\frac{\alpha_m}{\sqrt{\lambda_{i+1}}}\, r_{i+1}\right) - J_1\!\left(\frac{\alpha_m}{\sqrt{\lambda_i}}\, r_i\right) Y_0\!\left(\frac{\alpha_m}{\sqrt{\lambda_{i+1}}}\, r_{i+1}\right)\right\},$$

$$DET = J_0\!\left(\frac{\alpha_m}{\sqrt{\lambda_i}}\, r_i\right) Y_1\!\left(\frac{\alpha_m}{\sqrt{\lambda_i}}\, r_i\right) - Y_0\!\left(\frac{\alpha_m}{\sqrt{\lambda_i}}\, r_i\right) J_1\!\left(\frac{\alpha_m}{\sqrt{\lambda_i}}\, r_i\right).$$

Therefore, the eigenvalues α_m are determined from Eq. (12) and the homogeneous boundary conditions at the inside and outside surface, and the corresponding eigenfunctions for all layers are determined from Eq. (12).

2.4 Thermal stress analysis

We consider the unsteady thermal stresses in a FGM hollow circular cylinder due to the two-dimensional unsteady temperature change along both the r- and z-axis. We assume that the mechanical boundary conditions are traction free and that there is symmetry along the z-axis as follows:

$$\sigma_{rr}(r_a, z) = \sigma_{rz}(r_a, z) = 0 \quad \text{at} \quad r = r_a\,, \qquad 0 < z < \infty\,, \tag{13.1}$$

$$\sigma_{rr}(r_b, z) = \sigma_{rz}(r_b, z) = 0 \quad \text{at} \quad r = r_b\,, \qquad 0 < z < \infty\,. \tag{13.2}$$

When the material properties are functions of the r-directional position, the two-dimensional basic equation for the thermal stress of a FGM hollow circular cylinder without external forces is as follows:

$$\Delta^2\Delta^2 M_i(r,z) = 0 \quad \text{at} \quad r_{i-1} \le r \le r_i\,, \qquad i = 1,2,\ldots,L\,, \tag{14}$$

$$\nabla^2\phi_i(r,z,t) = \frac{1+\nu_i}{1-\nu_i}\,\alpha_i\{T_i^s(r,z) + \theta_i(r,z,t)\} \quad \text{at} \quad r_{i-1} \le r \le r_i\,, \qquad i = 1,2,\ldots,L\,, \tag{15}$$

where $M_i(r,z)$ and $\phi_i(r,z,t)$ denote Michell's function [17] and Goodier's thermoelastic displacement potential function [18], respectively, and α_i and ν_i are the coefficient of linear thermal expansion and Poisson's ratio of the i-th layer, respectively.

Considering the form of the temperature, we can obtain the solution of Eq. (14) as:

$$M_i(r,z) = \int_0^\infty [I_0(\beta r)\, E_i + K_0(\beta r)\, F_i + r I_1(\beta r)\, P_i + r K_1(\beta r)\, Q_i]\, \sin(\beta z)\, d\beta\,, \tag{16}$$

where I_0, K_0, I_1 and K_1 are the modified Bessel functions, respectively, and $E_i(\beta), F_i(\beta), P_i(\beta)$ and $Q_i(\beta)$ are coefficients to be evaluated.

Finally, we can obtain the solution of Eq. (15) as

$$\begin{aligned}\phi_i(r,z,t) = {} & \left(\frac{1+\nu_i}{1-\nu_i}\,\alpha_i\right)\int_0^\infty \frac{1}{2\beta}\,\{r I_1(\beta r)\, A_i - r K_1(\beta r)\, B_i\}\, \cos(\beta z)\, d\beta \\ & - \left(\frac{1+\nu_i}{1-\nu_i}\,\alpha_i\right)\sum_{m=1}^\infty \int_0^\infty \frac{\lambda_i C_m(\beta)}{\alpha_m^2 + \lambda_i\beta^2}\, \varphi_{im}(\alpha_m, r)\, \cos(\beta z)\, e^{-(\alpha_m^2+\lambda_i\beta^2)t}\, d\beta\,. \end{aligned} \tag{17}$$

Thus, we can obtain the thermal stresses and displacements in the i-th layer as:

$$(\sigma_{rr})_i = 2G_i\left[\frac{\partial}{\partial z}\left(\nu_i \Delta^2 M_i - \frac{\partial^2 M_i}{\partial r^2}\right) + \frac{\partial^2 \phi_i}{\partial r^2} - \frac{1+\nu_i}{1-\nu_i}\,\alpha_i(T_i^s + \theta_i)\right], \tag{18.1}$$

$$(\sigma_{\theta\theta})_i = 2G_i\left[\frac{\partial}{\partial z}\left(\nu_i \Delta^2 M_i - \frac{\partial^2 M_i}{r\partial r}\right) + \frac{\partial \phi_i}{r\partial r} - \frac{1+\nu_i}{1-\nu_i}\,\alpha_i(T_i^s + \theta_i)\right], \tag{18.2}$$

$$(\sigma_{zz})_i = 2G_i\left[\frac{\partial}{\partial z}\left\{(2-\nu_i)\,\Delta^2 M_i - \frac{\partial^2 M_i}{\partial z^2}\right\} + \frac{\partial^2 \phi_i}{\partial z^2} - \frac{1+\nu_i}{1-\nu_i}\,\alpha_i(T_i^s + \theta_i)\right], \tag{18.3}$$

$$(\sigma_{rz})_i = 2G_i\left[\frac{\partial}{\partial r}\left\{(1-\nu_i)\,\Delta^2 M_i - \frac{\partial^2 M_i}{\partial z^2}\right\} + \frac{\partial^2 \phi_i}{\partial r\partial z}\right], \tag{18.4}$$

$$(u_r)_i = \frac{\partial \phi_i}{\partial r} - \frac{\partial^2 M_i}{\partial r\partial z}, \tag{18.5}$$

$$(u_z)_i = \frac{\partial \phi_i}{\partial z} + 2(1-\nu_i)\,\Delta^2 M_i - \frac{\partial^2 M_i}{\partial z^2}, \tag{18.6}$$

where G_i is the shear modulus.

The unknown coefficients E_i, F_i, P_i, Q_i given in Eq. (16) are determined so that Eqs. (18) should satisfy the mechanical boundary conditions given in Eqs. (13) and the following continuity conditions of stresses and displacements:

$$(\sigma_{rr})_i = (\sigma_{rr})_{i+1} \quad \text{at} \quad r = r_i\,, \qquad i = 1,2,\dots,(L-1) \tag{19.1}$$

$$(\sigma_{rz})_i = (\sigma_{rz})_{i+1} \quad \text{at} \quad r = r_i\,, \qquad i = 1,2,\dots,(L-1) \tag{19.2}$$

$$(u_r)_i = (u_r)_{i+1} \quad \text{at} \quad r = r_i\,, \qquad i = 1,2,\dots,(L-1) \tag{19.3}$$

$$(u_z)_i = (u_z)_{i+1} \quad \text{at} \quad r = r_i\,, \qquad i = 1,2,\dots,(L-1)\,. \tag{19.4}$$

3 Numerical results and discussion

Numerical calculations are carried out for a FGM hollow circular cylinder with an infinite length made of zirconium oxide and titanium alloy. The material properties, the volumetric ratio of the metal, $V_m = (1 + \bar{R}_a - \bar{R})^M$, and the porosity as a function of the position $P = A_p(\bar{R} - \bar{R}_a)\,(1 + \bar{R}_a - \bar{R})$ are used in Ref. [1], respectively. $\bar{R}$ denotes the dimensionless position defined by $\bar{R} = r/(r_b - r_a)$.

As an illustrative example, we consider that the inside and outside surfaces of the cylinder are subjected to partial heating as follows:

$$T_a(\bar{z}) = T_0 + T_1 \cos(\pi\bar{z}/2) \quad \text{at} \quad \bar{R} = \bar{R}_a\big(= r_a/(r_b - r_a)\big)\,, \qquad 0 \le \bar{z} \le 1\,,$$

$$T_b(\bar{z}) = T_0 + T_2 \cos(\pi\bar{z}/2) \quad \text{at} \quad \bar{R} = \bar{R}_b\big(= r_b/(r_b - r_a)\big)\,, \qquad 0 \le \bar{z} \le 1\,,$$

$$T_a(\bar{z}) = T_b(\bar{z}) = T_0 \quad \text{at} \quad \bar{R} = \bar{R}_a = \bar{R}_b\,, \qquad \bar{z} \ge 1\,,$$

where T_0, T_1 and T_2 denote the initial and arbitrary temperatures, respectively.

For the numerical calculations, we used the dimensionless quantities as follows:

$$\bar{T} = (T - T_0)/T_0\,, \qquad \bar{z} = z/(r_b - r_a)\,, \qquad \tau = \lambda_m t/(r_b - r_a)^2\,,$$

where $\bar{T}, \bar{z}, \tau$ and λ_m denote the dimensionless temperature, the dimensionless position in the z-direction, the Fourier number and the thermal diffusivity of the metal, respectively.

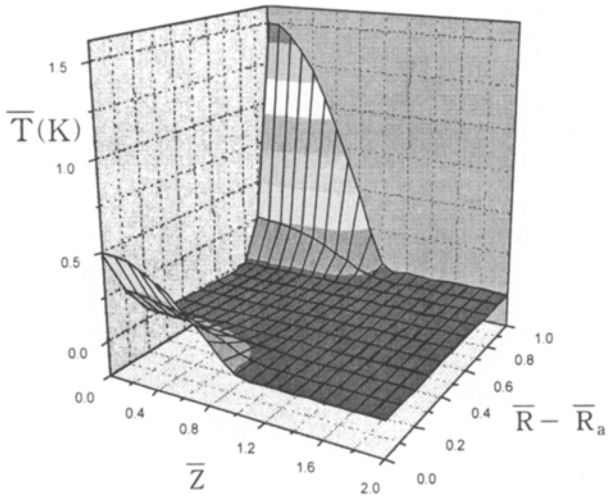

Fig. 1. Unsteady dimensionless temperature distribution with dimensionless position at $\tau = 0.01$ ($T_1 = 0.5$ K, $T_2 = 1.5$ K, $T_0 = 1.0$ K, $\bar{R}_a = 5$, $M = 1$, $P = 0$)

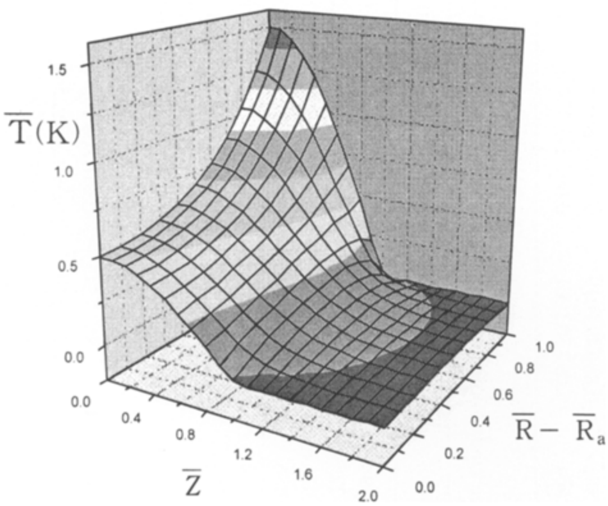

Fig. 2. Unsteady dimensionless temperature distribution with dimensionless position at $\tau = \infty$, ($T_1 = 0.5$ K, $T_2 = 1.5$ K, $T_0 = 1.0$ K, $\bar{R}_a = 5$, $M = 1$, $P = 0$)

Figures 1 and 2 show the dimensionless temperature distribution of a FGM hollow circular cylinder with dimensionless position. After checking the convergence of the series in the temperature solution, the truncated numbers of the series are selected as $m = 50$, and the number of layers $L = 50$ is used in Eq. (9).

Tables 1 and 2 show the convergence of the thermal stresses with the number of layers L at two kinds of the Fourier number, respectively. The convergence of the steady solution is faster than that of the unsteady solution, but the convergence of the solution at the small Fourier number $\tau = 0.01$ requires many layers in order to achieve a high degree of accuracy.

Tables 3 and 4 show the convergence of the thermal stresses with the number of eigenvalues m at two kinds of the Fourier number, respectively. The convergence of the steady and unsteady solution is very fast, and the effect of the number of eigenvalues is small in comparison with that of the number of layers. When the truncated numbers of series and the number of layers are selected as $m = 50$ and $L = 150$, it can be considered that sufficient convergence for the solution is achieved.

Figures 3–6 show the variation of the unsteady thermal stress distribution versus the dimensionless radial position for different values of the Fourier number in a two-dimensional

Table 1. Thermal stresses versus the number of layer L for three kinds of dimensionless position at $\tau = \infty$ ($m = 50$, $T_1 = 0.5$ K, $T_2 = 1.5$ K, $\bar{R}_a = 5$, $M = 1$, $P = 0$)

The number of Layer L		20	30	40	50	60	70	200
$\bar{R} - \bar{R}_a = 0.5$, $\bar{z} = 0.1$	σ_{rr}	0.045 271 137	0.045 264 406	0.045 262 016	0.045 260 906	0.045 260 302	0.045 259 937	0.045 259 053
	σ_{rz}	−0.014 427 843	−0.014 442 862	−0.014 448 104	−0.014 450 528	−0.014 451 844	−0.014 452 638	−0.014 454 566
	$\sigma_{\theta\theta}$	−0.283 979 244	−0.284 105 355	−0.284 149 517	−0.284 169 957	−0.284 181 060	−0.284 187 753	−0.284 204 012
	σ_{zz}	0.106 809 319	0.106 590 268	0.106 513 606	0.106 478 126	0.106 458 856	0.106 447 237	0.106 419 010
$\bar{R} - \bar{R}_a = 0.9$, $\bar{z} = 0.1$	σ_{rr}	0.024 767 040	0.024 770 704	0.024 772 309	0.024 773 148	0.024 773 636	0.024 773 943	0.024 774 730
	σ_{rz}	0.000 098 926	0.000 091 202	0.000 088 389	0.000 087 057	0.000 086 324	0.000 085 879	0.000 084 785
	$\sigma_{\theta\theta}$	−1.217 867 640	−1.218 056 500	−1.218 122 237	−1.218 152 585	−1.218 169 046	−1.218 178 963	−1.218 203 025
	σ_{zz}	−0.075 228 745	−0.075 582 517	−0.075 706 154	−0.075 763 344	−0.075 794 399	−0.075 813 119	−0.075 858 584
$\bar{R} - \bar{R}_a = 0.9$, $\bar{z} = 0.5$	σ_{rr}	0.016 610 350	0.016 619 632	0.016 622 697	0.016 624 085	0.016 624 830	0.016 625 277	0.016 626 358
	σ_{rz}	0.000 581 864	0.000 526 077	0.000 506 921	0.000 498 131	0.000 493 378	0.000 490 520	0.000 483 603
	$\sigma_{\theta\theta}$	−0.806 291 871	−0.806 427 588	−0.806 475 019	−0.806496 959	−0.806 508 873	−0.806 516 054	−0.806 533 494
	σ_{zz}	−0.096 968 104	−0.097 215 604	−0.097 302 261	−0.097 342 374	−0.097 364 163	−0.097 377 300	−0.097 409 214

Table 2. Thermal stresses versus the number of layer L for three kinds of dimensionless position at $\tau = 0.01$ ($m = 50$, $T_1 = 0.5$ K, $T_2 = 1.5$ K, $\bar{R}_a = 5$, $M = 1$, $P = 0$)

The number of Layer L		140	150	160	170	180	190	200
$\bar{R} - \bar{R}_a = 0.5$, $\bar{z} = 0.1$	σ_{rr}	−0.004 993 104	−0.004 990 594	−0.004 988 527	−0.004 986 461	−0.004 984 220	−0.004 982 670	0.004 981 273
	σ_{rz}	−0.012 591 238	−0.012 591 227	−0.012 591 213	−0.012 591 198	−0.012 591 235	−0.012 591 227	−0.012 591 219
	$\sigma_{\theta\theta}$	−0.837 109 164	−0.837 111 976	−0.837 114 472	−0.837 116 967	−0.837 079 045	−0.837 080 632	−0.837 082 052
	σ_{zz}	−0.397 967 100	−0.397 969 486	−0.397 971 604	−0.397 973 722	−0.397 935 164	−0.397 936 448	−0.397 937 588
$\bar{R} - \bar{R}_a = 0.9$, $\bar{z} = 0.1$	σ_{rr}	0.015 217 566	0.015 209 815	0.015 203 439	0.015 197 063	0.015 192 009	0.015 187 265	0.015 182 997
	σ_{rz}	−0.004 602 714	−0.004 603 002	−0.004 603 225	−0.004 603 448	−0.004 603 595	−0.004 603 742	−0.004 603 869
	$\sigma_{\theta\theta}$	−0.231 291 254	−0.231 290 902	−0.231 290 581	−0.231 290 259	−0.231 251 084	−0.231 250 902	−0.231 250 700
	σ_{zz}	0.719 269 231	0.719 265 404	0.719 262 397	0.719 259 389	0.719 296 978	0.719 294 766	0.719 292 840
$\bar{R} - \bar{R}_a = 0.9$, $\bar{z} = 0.5$	σ_{rr}	0.011 202 181	0.011 197 504	0.011 193 656	0.011 189 808	0.011 186 776	0.011 183 912	0.011 181 335
	σ_{rz}	−0.016 801 288	−0.016 802 408	−0.016 803 254	−0.016 804 100	−0.016 804 736	−0.016 805 269	−0.016 805 728
	$\sigma_{\theta\theta}$	−0.099 245 271	−0.099 244 772	−0.099 244 350	−0.099 243 925	−0.099 215 631	−0.099 215 349	−0.099 215 069
	σ_{zz}	0.502 750 634	0.502 747 960	0.502 745 843	0.502 743 721	0.502 770 644	0.502 769 089	0.502 767 734

Table 3. Thermal stresses versus the number of eigenvalues m for three kinds of dimensionless position at $\tau = \infty$ ($L = 50$, $T_1 = 0.5$ K, $T_2 = 1.5$ K, $\bar{R}_a = 5$, $M = 1$, $P = 0$)

The number of Eigenvalues m		10	50
$\bar{R} - \bar{R}_a = 0.5$, $\bar{z} = 0.1$	σ_{rr}	0.045 260 906	0.045 260 906
	σ_{rz}	−0.014 450 528	−0.014 450 528
	$\sigma_{\theta\theta}$	−0.284 169 957	−0.284 169 957
	σ_{zz}	0.106 478 126	0.106 478 126
$\bar{R} - \bar{R}_a = 0.9$, $\bar{z} = 0.1$	σ_{rr}	0.024 773 148	0.024 773 148
	σ_{rz}	0.000 087 057	0.000 087 057
	$\sigma_{\theta\theta}$	−1.218 152 585	−1.218 152 585
	σ_{zz}	−0.075 763 344	−0.075 763 344
$\bar{R} - \bar{R}_a = 0.9$, $\bar{z} = 0.5$	σ_{rr}	0.016 624 085	0.016 624 085
	σ_{rz}	0.000 498 131	0.000 498 131
	$\sigma_{\theta\theta}$	−0.806 496 959	−0.806 496 959
	σ_{zz}	−0.097 342 374	−0.097 342 374

Table 4. Thermal stresses versus the number of eigenvalues m for three kinds of dimensionless position at $\tau = 0.01$ ($L = 150$, $T_1 = 0.5$ K, $T_2 = 1.5$ K, $\bar{R}_a = 5$, $M = 1$, $P = 0$)

The number of Eigenvalues m		10	20	30	40	50
$\bar{R} - \bar{R}_a = 0.5$, $\bar{z} = 0.1$	σ_{rr}	−0.004 990 571	−0.004 990 594	−0.004 990 594	−0.004 990 594	−0.004 990 594
	σ_{rz}	−0.012 591 250	−0.012 591 227	−0.012 591 227	−0.012 591 227	−0.012 591 227
	$\sigma_{\theta\theta}$	−0.837 114 726	−0.837 111 976	−0.837 111 976	−0.837 111 976	−0.837 111 976
	σ_{zz}	−0.397 972 296	−0.397 969 486	−0.397 969 486	−0.397 969 486	−0.397 969 486
$\bar{R} - \bar{R}_a = 0.9$, $\bar{z} = 0.1$	σ_{rr}	0.015 209 839	0.015 209 815	0.015 209 815	0.015 209 815	0.015 209 815
	σ_{rz}	−0.004 603 013	−0.004 603 002	−0.004 603 002	−0.004 603 002	−0.004 603 002
	$\sigma_{\theta\theta}$	−0.231 288 367	−0.231 290 902	−0.231 290 902	−0.231 290 902	−0.231 290 902
	σ_{zz}	0.719 268 104	0.719 265 404	0.719 265 404	0.719 265 404	0.719 265 404
$\bar{R} - \bar{R}_a = 0.9$, $\bar{z} = 0.5$	σ_{rr}	0.011 197 520	0.011 197 504	0.011 197 504	0.011 197 504	0.011 197 504
	σ_{rz}	−0.016 802 477	−0.016 802 408	−0.016 802 408	−0.016 802 408	−0.016 802 408
	$\sigma_{\theta\theta}$	−0.099 242 961	−0.099 244 772	−0.099 244 772	−0.099 244 772	−0.099 244 772
	σ_{zz}	0.502 749 858	0.502 747 960	0.502 747 960	0.502 747 960	0.502 747 960

FGM and homogeneous hollow circular cylinder, respectively. In these figures, the distribution and values of hoop stress $\sigma_{\theta\theta}$ and axial stress σ_{zz} are similar, but the distributions of the radial stress σ_{rr} and shear stress σ_{rz} are different from them, and these values are much smaller than those of $\sigma_{\theta\theta}$ and σ_{zz} at the same Fourier number. Thus, hoop stress $\sigma_{\theta\theta}$ and axial stress σ_{zz} are the governing stresses in a FGM and homogeneous hollow circular cylinder, and it is shown that these unsteady compressive stresses at the ceramic side are greater than that of the steady state.

Figures 7–12 show the two-dimensional unsteady thermal stress distributions with the dimensionless position for the Fourier numbers $\tau = 0.01$ and $\tau = \infty$, respectively. Hoop stress $\sigma_{\theta\theta}$ and axial stress σ_{zz} at the heated surface are changed significantly according to the varia-

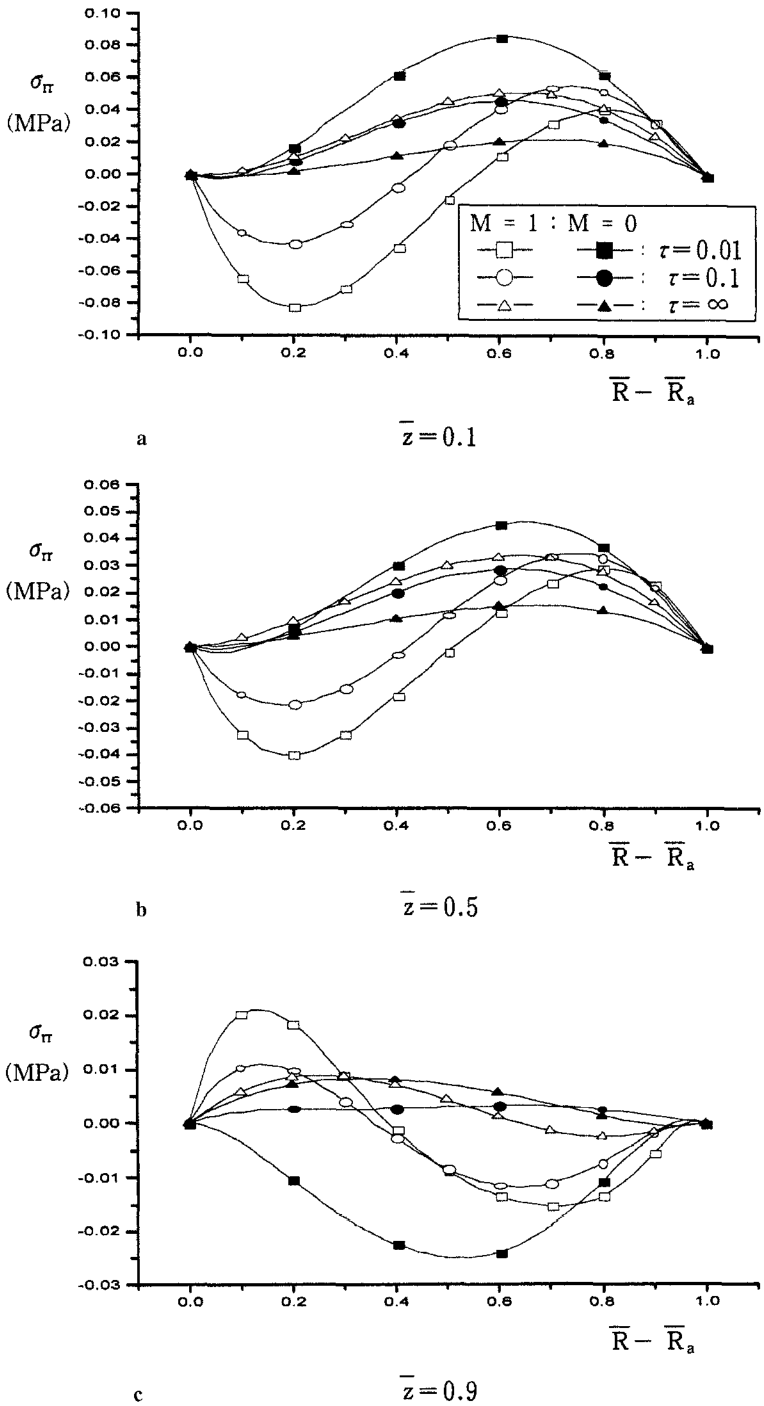

Fig. 3. Thermal stress σ_{rr} of a FGM and homogeneous hollow circular cylinder ($T_1 = 0.5$ K, $T_2 = 1.5$ K, $\bar{R}_a = 5$, $P = 0$)

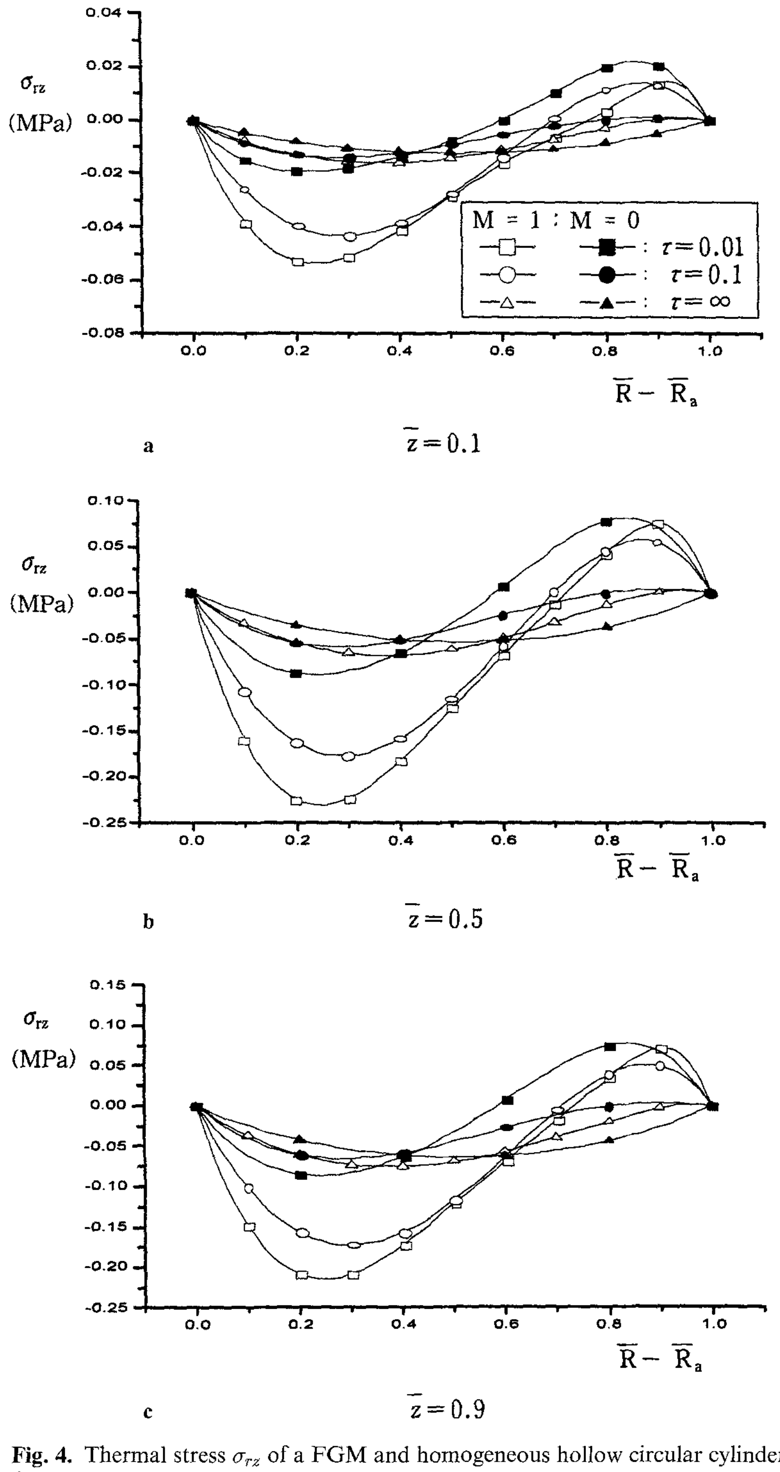

Fig. 4. Thermal stress σ_{rz} of a FGM and homogeneous hollow circular cylinder ($T_1 = 0.5$ K, $T_2 = 1.5$ K, $\bar{R}_a = 5$, $P = 0$)

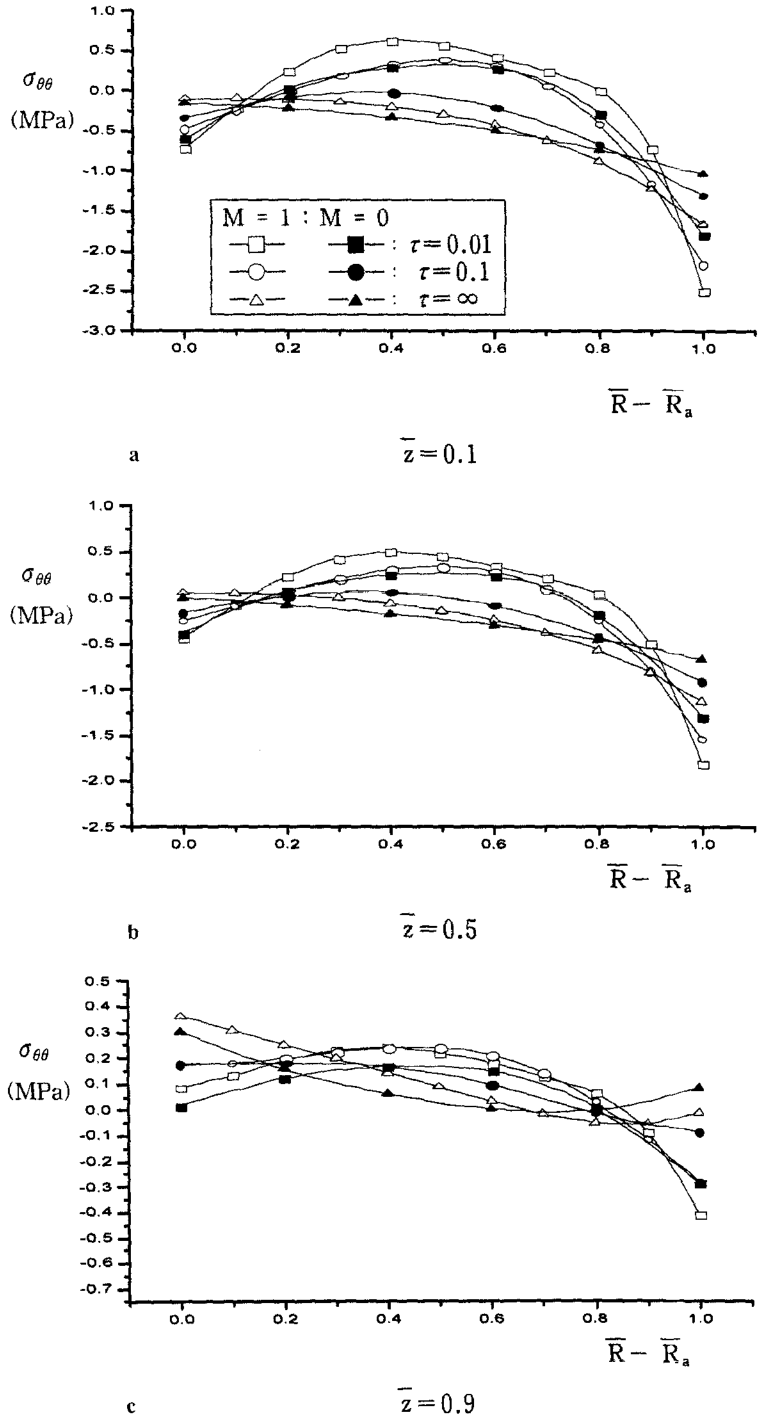

Fig. 5. Thermal stress $\sigma_{\theta\theta}$ of a FGM and homogeneous hollow circular cylinder ($T_1 = 0.5$ K, $T_2 = 1.5$ K, $\bar{R}_a = 5$, $P = 0$)

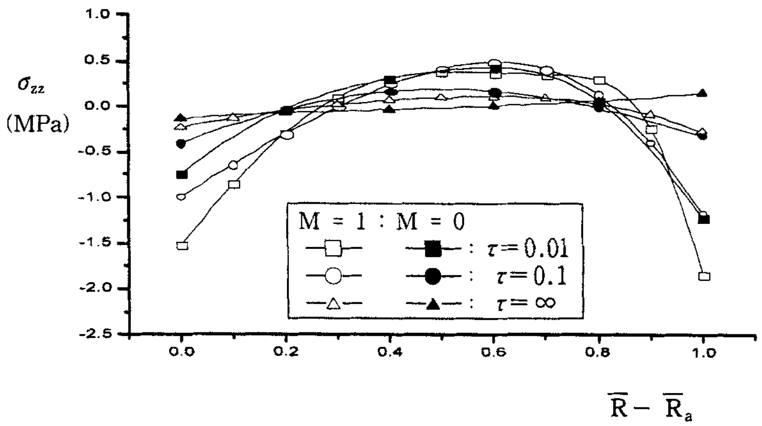

a $\bar{z} = 0.1$

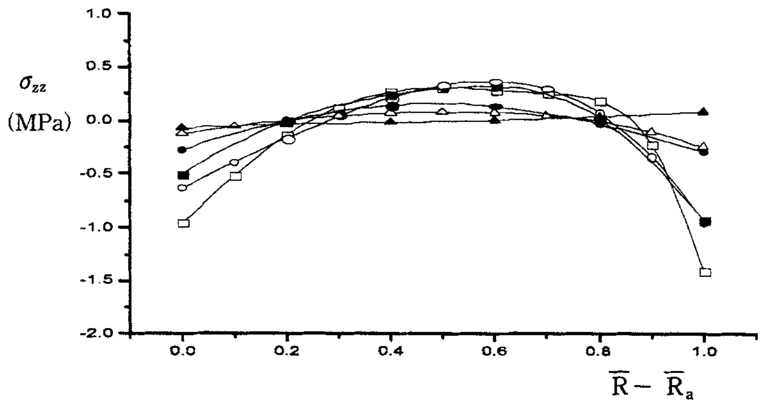

b $\bar{z} = 0.5$

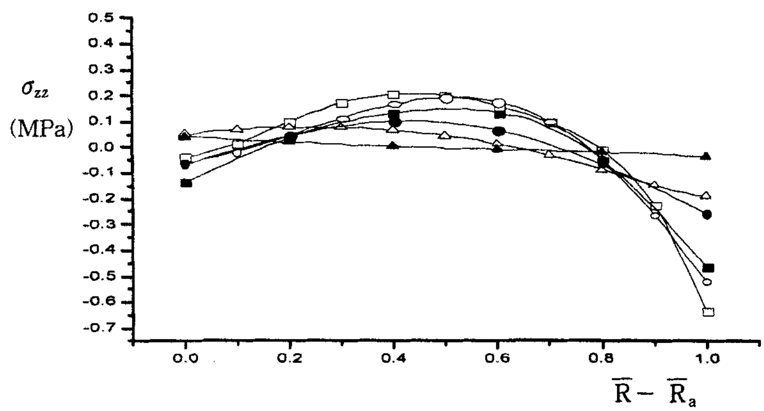

c $\bar{z} = 0.9$

Fig. 6. Thermal stress σ_{zz} of a FGM and homogeneous hollow circular cylinder ($T_1 = 0.5$ K, $T_2 = 1.5$ K, $\bar{R}_a = 5$, $P = 0$)

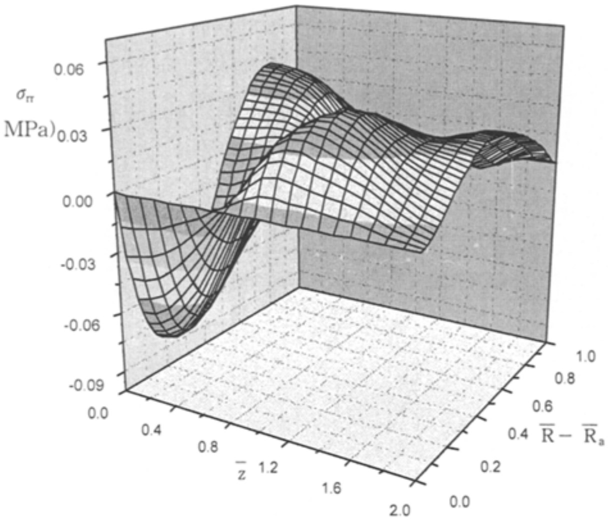

Fig. 7. Two-dimensional unsteady thermal stress distributions σ_{rr} with dimensionless position at $\tau = 0.01$ ($T_1 = 0.5\,\mathrm{K}$, $T_2 = 1.5\,\mathrm{K}$, $\bar{R}_a = 5$, $M = 1$, $P = 0$)

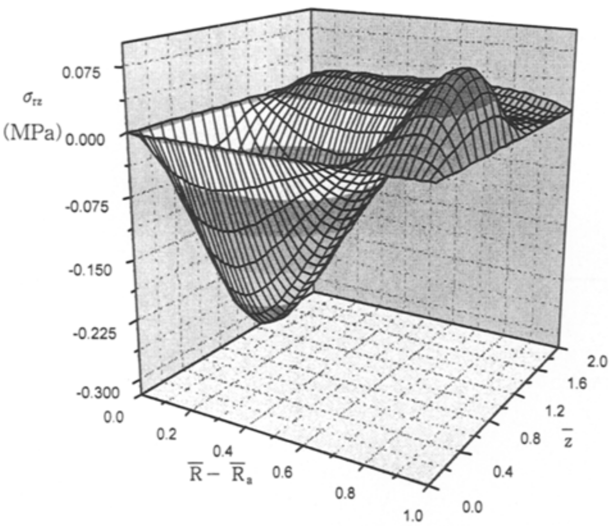

Fig. 8. Two-dimensional unsteady thermal stress distributions σ_{rz} with dimensionless position at $\tau = 0.01$ ($T_1 = 0.5\,\mathrm{K}$, $T_2 = 1.5\,\mathrm{K}$, $\bar{R}_a = 5$, $M = 1$, $P = 0$)

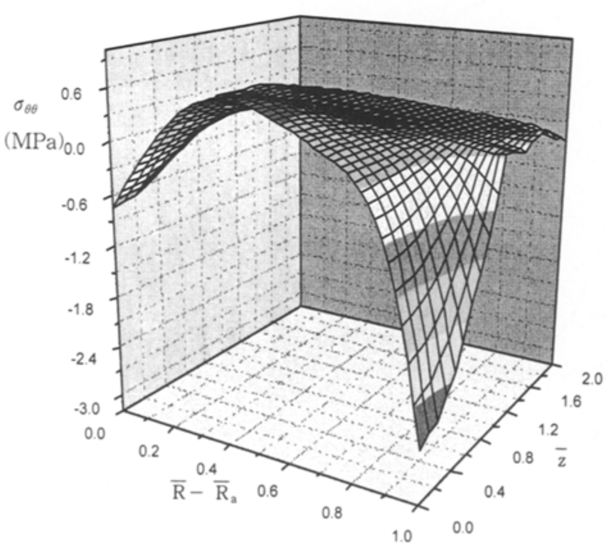

Fig. 9. Two-dimensional unsteady thermal stress distributions $\sigma_{\theta\theta}$ with dimensionless position at $\tau = 0.01$ ($T_1 = 0.5\,\mathrm{K}$, $T_2 = 1.5\,\mathrm{K}$, $\bar{R}_a = 5$, $M = 1$, $P = 0$)

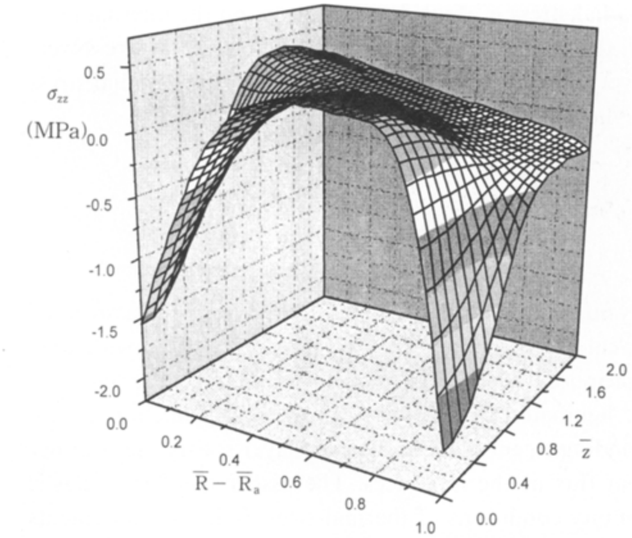

Fig. 10. Two-dimensional unsteady thermal stress distributions σ_{zz} with dimensionless position at $\tau = 0.01$ ($T_1 = 0.5\,\mathrm{K}$, $T_2 = 1.5\,\mathrm{K}$, $\bar{R}_a = 5$, $M = 1$, $P = 0$)

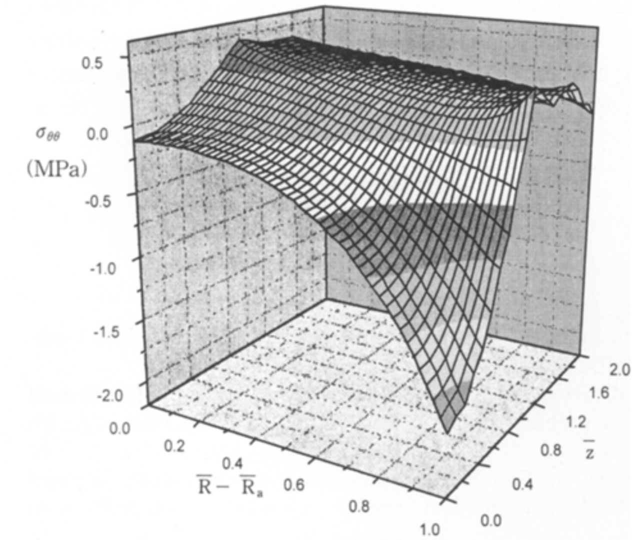

Fig. 11. Two-dimensional unsteady thermal stress distributions $\sigma_{\theta\theta}$ with dimensionless position at $\tau = \infty$ ($T_1 = 0.5\,\mathrm{K}$, $T_2 = 1.5\,\mathrm{K}$, $\bar{R}_a = 5$, $M = 1$, $P = 0$)

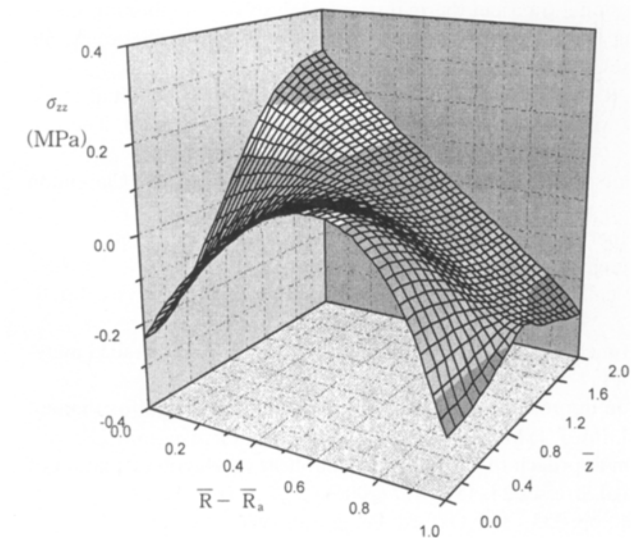

Fig. 12. Two-dimensional unsteady thermal stress distributions σ_{rz} with dimensionless position at $\tau = \infty$ ($T_1 = 0.5\,\mathrm{K}$, $T_2 = 1.5\,\mathrm{K}$, $\bar{R}_a = 5$, $M = 1$, $P = 0$)

tion of the dimensionless time, while radial stress σ_{rr} and shear stress σ_{rz} on the internal position are changed significantly. That is, the maximum compressive hoop and axial stress were produced on the ceramic surface at a very small time, while the maximum tensile radial stress occurs on the internal position of the cylinder.

3 Conclusions

A Green's function approach for analyzing the unsteady temperature field and the associated thermoelastic field in a two-dimensional FGM hollow circular infinite cylinder with one-directionally dependent properties is proposed. Green's functions for analyzing the temperature field are formulated by using the laminate theory and the proper eigenfunction expansion. The eigenvalues and the corresponding eigenfunctions for each layer satisfy the continuity conditions of temperature and heat flux at the interfaces. The associated thermoelastic field is formulated to satisfy the continuity conditions of thermal stresses and displacements at the interfaces with Michell's function and the thermoelastic displacement potential function. Therefore, by a comparison of the numerical results with the number of layers, we show that the proposed method is simple and accurate. The proposed method has a potential of being used to aid the calculation of the optimum material distribution in a FGM hollow circular cylinder.

References

[1] Tanigawa, Y.: Some basic thermoelastic problems for nonhomogeneous structural materials. Trans. ASME, J. Appl. Mech. **48,** 287–300 (1995).
[2] Obata, Y., Noda, N.: Unsteady thermal stresses in a functionally gradient material plate (Analysis of one-dimensional unsteady heat transfer problem). Trans. Japan Soc. Mech. Eng., Series A, **59,** No. 560, 1090–1096 (1993) (in Japanese).
[3] Obata, Y., Kanayama, K., Ohji, T., Noda, N.: Two-dimensional unsteady thermal stresses in a partially heated circular cylinder made of functionally gradient materials. 3rd Int. Congress on Thermal Stresses, pp. 595–598 (1999).
[4] Ootao, Y., Tanigawa, Y.: Three-dimensional transient thermal stress analysis of a nonhomogeneous hollow sphere with respect to rotating heat source. Trans. Japan Soc. Mech. Eng., Series A, **60,** No. 578, 2273–2279 (1994) (in Japanese).
[5] Tanigawa, Y., Akai, T., Kawamura, R., Oka, N.: Transient heat conduction and thermal stress problems of a nonhomogeneous plate with temperature-dependent material properties. J. Thermal Stresses **19,** 77–102 (1996).
[6] Carslaw, H. S., Jaeger, J. C.: Conduction of heat in solids, 2nd ed., pp. 352–386. Oxford: Clarendon Press 1959.
[7] Boley, B. A., Weiner, J. H.: Theory of thermal stresses, pp. 179–183. New York: Wiley 1960.
[8] Parkus, H.: Instationäre Wärmespannungen, pp. 18–71. Wien: Springer 1959.
[9] Diaz, R., Nomura, S.: Numerical Green's function approach to finite-sized plate analysis. Int. J. Solids Struct. **33,** 4215–4222 (1996).
[10] Nomura, S., Sheahen, D. M.: Green's function approach to the analysis of functionally graded materials. ASME MD-80, pp. 19–23 (1997).
[11] Kim, K. S., Noda, N.: Green's function approach to solution of transient temperature for thermal stresses of functionally graded material. Int. J. JSME, Series A, **44,** 31–36 (2001).
[12] Kim, K. S., Noda, N.: Green's function approach to three-dimensional heat conduction equation of functionally graded materials. J. Thermal Stresses **24,** 457–477 (2001).
[13] Nowacki, W.: Thermoelasticity, 2nd ed., pp. 333–355. Oxford: Pergamon 1986.

[14] Obata, Y., Noda, N.: Steady thermal stresses in a hollow circular cylinder and a hollow sphere of a functionally gradient material. J. Thermal Stresses **17,** 471 – 487 (1994).

[15] Ootao, Y., Akai, T., Tanigawa, Y.: Three-dimensional transient thermal stress analysis of a nonhomogeneous hollow circular cylinder due to a moving heat source in axial direction. J. Thermal Stresses **18,** 497 – 512 (1995).

[16] Tanigawa, Y., Oka, N., Kawamura, R., Akai, T.: One-dimensional transient thermal stress problem for nonhomogeneous hollow circular cylinder and its optimization of material composition for thermal stress relaxation. JSME Int. J., Ser. A, **40,** 117 – 127 (1997).

[17] Goodier, J. N.: Integration of thermoelastic equations. Phil. Mag. **23,** 1017 (1937).

[18] Michell, J. H.: On the direct determination of stress in an elastic solid, with application to the theory of plates. Proc. London Math. Soc. **31,** 100 – 124 (1899).

[19] Ozisik, M. N.: Heat conduction, pp. 47 – 54. New York: Wiley 1993.

Authors' addresses: Dr. K.-S. Kim, Department of Aeronautical Engineering, Inha Technical College, 253 Yonghyun-dong Nam-ku, Incheon, 402-752, Korea (E-mail: kuiseob@true.inhatc.ac.kr); Prof. N. Noda, Department of Mechanical Engineering, Shizuoka University, 3-5-1 Johoku Hamamatsu, 432-8561, Japan (E-mail: tmnnoda@ipc.shizuoka.ac.jp)